



Contents lists available at ScienceDirect

Organic Geochemistry

journal homepage: www.elsevier.com/locate/orggeochem

An irrigation experiment to compare soil, water and speleothem tetraether membrane lipid distributions



Andy Baker^{a,*}, Catherine N. Jex^a, Helen Rutledge^{a,b}, Martijn Woltering^c, Alison J. Blyth^d, Martin S. Andersen^e, Mark O. Cuthbert^{e,f}, Christopher E. Marjo^b, Monika Markowska^{a,g}, Gabriel C. Rau^e, Stuart J. Khan^h

^a Connected Waters Initiative Research Centre, UNSW Australia, NSW 2052, Australia

^b Solid State and Elemental Analysis Unit, Mark Wainwright Analytical Centre, UNSW Australia, Kensington, NSW 2052, Australia

^c CSIRO, Mineral Resources Flagship, Perth, WA 6151, Australia

^d WA-OIGC, Department of Chemistry, Chemistry and Resources Precinct, Curtin University, GPO Box U1987, Perth, WA 6845, Australia

^e Connected Waters Initiative Research Centre, UNSW Australia, 110 King Street, Manly Vale, NSW 2093, Australia

^f School of Geography, Earth and Environmental Sciences, University of Birmingham, Edgbaston, Birmingham B15 2TT, UK

^g Australian Nuclear Science and Technology Organisation, Lucas Heights, NSW 2234, Australia

^h School of Civil and Environmental Engineering, UNSW Australia, NSW 2052, Australia

ARTICLE INFO

Article history:

Received 10 August 2015

Received in revised form 23 December 2015

Accepted 7 January 2016

Available online 25 January 2016

Keywords:

GDGT

Speleothem

Drip water

Paleoclimate

Temperature

ABSTRACT

Measurement of glycerol dialkyl glycerol tetraethers (GDGTs) preserved in speleothems offers a potential proxy for past temperature but, in general, their origin is unknown. To understand the source of speleothem GDGTs, we undertook an irrigation experiment to activate drip sites within a hydrogeochemically well characterised cave. The cave drip water was analysed for GDGTs, inorganic elements (major ions and trace elements), stable isotopes and dissolved organic matter concentration and character. Published speleothem GDGT records from the site have been observed to be dominated by isoprenoid GDGTs and interpreted as deriving from in situ microbial communities within the cave or vadose zone. The drip water in our irrigation experiment had a GDGT distribution distinct from that of soil and speleothem samples, providing direct evidence that the distinctive GDGT signature in speleothems is derived from a subsurface source. Analysis of GDGTs in this context allowed further elucidation of their source and transport in cave systems, enhancing our understanding of how they might be used as a temperature proxy.

© 2016 Elsevier Ltd. All rights reserved.

1. Introduction

There has been increasing interest in dissolved organic matter (DOM) in cave drip water and the potential use of organic markers in speleothems as paleoclimate proxies (Blyth et al., 2008; Fairchild and Baker, 2012). While initial studies focussed on fluorescent OM (Baker et al., 1997), subsequent investigations have focussed on the potential of lipid biomarkers (Xie et al., 2003; Blyth et al., 2007, 2011; Rushdi et al., 2011), $\delta^{13}\text{C}$ measurements of OM (Blyth et al., 2013a,b; Li et al., 2014), lignin phenols (Blyth and Watson 2009; Blyth et al., 2010) and trace elements associated with organic colloids (Hartland et al., 2012). Lipids such as *n*-alkanes have been shown to record vegetation and land use change (Blyth et al. 2007, 2011) and glycerol dialkyl glycerol

tetraethers (GDGTs) have shown potential as a palaeotemperature proxy (Yang et al., 2011; Blyth and Schouten, 2013; Blyth et al., 2014).

GDGTs are widely used as a palaeoenvironmental proxy, predominantly for temperature reconstruction from lake and ocean sediments and soils (Schouten et al., 2013). They are divided into two classes. One, containing isoprenoid alkyl moieties (iGDGTs), is produced by Crenarchaeota, Thaumarchaeota and Euryarchaeota; the second comprises methyl branched alkyl chains with 0–2 cyclopentane moieties (brGDGTs) and is believed to be produced by bacteria (Schouten et al., 2013). These branched compounds were originally considered to be associated with soil derived terrigenous input, although recent studies have now found that they can also be produced in situ in aquatic environments (for a review see Schouten et al., 2013). The brGDGTs are more abundant than iGDGTs in soil (e.g. Weijers et al., 2006; Naeher et al., 2014). Ajioka et al. (2014) investigated GDGT depth profiles in soil

* Corresponding author.

E-mail address: a.baker@unsw.edu.au (A. Baker).

in the Lake Biwa basin and found that the maximum brGDGT concentration occurred in the surface organic ('O') horizon, decreasing with depth. In contrast, iGDGTs increased with depth. Huguët et al. (2014) demonstrated that, in a peat soil, brGDGTs had a turnover of at least 1 yr and that the source organisms rapidly (between 3 months and 1 yr) adjusted their membrane lipid composition to their environment. Weijers et al. (2010) used a natural labelling experiment using a change between C₃ and C₄ crop types to determine a turnover time of ca. 18 yr for brGDGTs in arable soil.

In soil, branching ratios have been shown to relate to temperature and pH (Weijers et al., 2007; Peterse et al., 2012). Blyth and Schouten (2013) and Blyth et al. (2014) have also demonstrated that a temperature signal is contained within GDGTs preserved in speleothems. In that case, the GDGTs were dominated by iGDGTs, despite the drip water supplying the speleothems initially having a soil source and, in most cases, both the iGDGTs and brGDGTs had distinct compositions compared with overlying soil (Blyth et al., 2014). Blyth et al. (2014) hypothesised that the GDGTs in speleothems derive predominantly from a source further down the transport pathway from the soil, although comparison of speleothems and soils could not distinguish whether the source was in situ in the cave itself or derived from the vadose zone of the limestone.

To understand the processes determining the GDGTs in speleothems and to examine sources and transport of the compounds during a controlled recharge event, we used an artificial irrigation experiment. The site had been used for an artificial irrigation experiment in January 2013 that determined the karst hydrogeochemical

processes occurring from surface to cave (Rutledge et al., 2014). This and subsequent irrigation experiments in January and June 2014 were undertaken to improve understanding of various cave processes and potential speleothem proxies. These included heat transport processes (Rau et al., 2015), evaporative cooling of drip water (Cuthbert et al., 2014b), water isotope evaporation and vadose zone flow paths (Markowska et al., 2016) and OM characterisation using liquid chromatography – organic carbon detection (LC-OCD; Rutledge et al., 2015). Here, we report the GDGT results obtained from the January 2014 irrigation experiment.

2. Material and methods

2.1. Study site

Cathedral Cave at Wellington Caves Reserve, NSW, Australia (32°37'S; 148°56'E) was the location for our irrigation experiments (Fig. 1). It formed within massive Devonian limestone (Johnson, 1975) and the irrigation site is close to the cave entrance. Overlying the limestone is a thin layer of red-brown soil, comprising clays, iron oxides, fine quartz sand and calcite nodules (Frank, 1971), with an aeolian contribution (Hesse and McTinish, 2003). The site is within a temperate semi-arid region, with a mean annual precipitation of 619 mm (1956–2005) and pan evaporation of 1825 mm (1956–2005) recorded nearby at Wellington (Bureau of Meteorology, 2015). There is a significant seasonal temperature variation, with the monthly mean maximum ranging from 15 °C

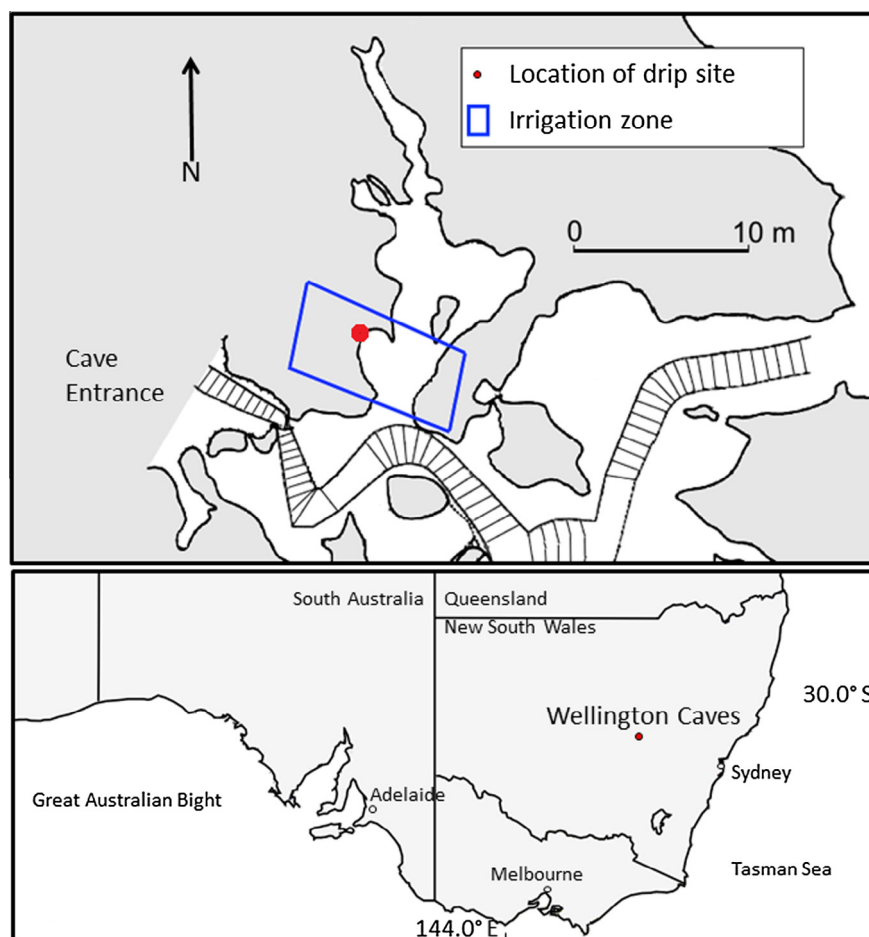


Fig. 1. Plan view of study site at Cathedral Cave, Wellington Caves (top), with a boxed area indicating where surface irrigation was performed, and location of the drip site (adapted from Sydney University Speleology Society survey map 2006–2007). Location of the study site in New South Wales in southeastern Australia (bottom).

in July to 32 °C in January. The cave is one of five sites reported by Blyth et al. (2014), whereby GDGT composition of soils and speleothems were compared.

Long term hydrogeological monitoring at the cave has helped elucidate recharge processes. Jex et al. (2012) described drip water patterns and processes and found that infiltration of drip water into the cave occurs only after rainfall events of high magnitude and long duration. A total precipitation of ca. 60 mm within 24–48 h is necessary, although this can vary depending on antecedent conditions. Such rainfall events occur very infrequently, typically 0–2 times a year (Cuthbert et al., 2014a). Drip water isotope monitoring has demonstrated that the $\delta^{18}\text{O}$ composition is dominated by epikarst evaporation (Cuthbert et al., 2014a). Due to the infrequency of recharge events, evaporation from near-surface karst water stores leads to enriched cave dripwater. This long term monitoring of drip water throughout the cave, combined with previous irrigation experiments at one location within the cave, has allowed a conceptual model of water movement at the irrigation site to be developed (Section 3.3).

2.2. Irrigation experiment

Details of the 2014 irrigation experiment have been described in detail elsewhere (Rutledge et al., 2015; Rau et al., 2015). An area of ca. 50 m², directly above the study area in the cave was evenly irrigated with Wellington town supply water. The experiment was performed at the height of summer (January 2014) and the antecedent soil moisture content in the top 10 cm of the soil within the irrigation area was relatively low (initial soil moisture $14.4 \pm 8.0\%$, $n = 10$), measured using trace micro-time domain reflectometry (TDR). Two irrigations by way of hand hosing were performed on consecutive mornings. Irrigation on Day 1 (Event 1) started at 7:50 am and continued for just under 3 h, until dripping started in the cave below the irrigation zone. A total of 3400 l

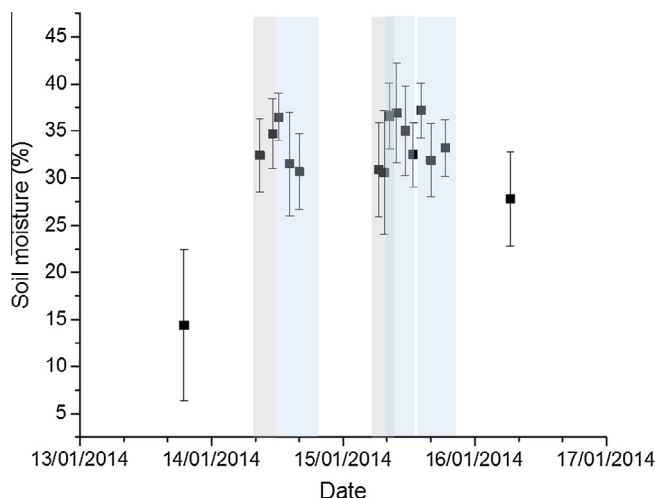


Fig. 3. Soil moisture content measured before, during and after the irrigation experiment using micro-TDR. The standard deviation variability is shown, based on ten TDR measurements within the irrigation zone. Grey shaded areas show timing of irrigation and blue shaded areas indicate timing of the three GDGT samples. (For interpretation of the references to colour in this figure legend, the reader is referred to the web version of this article.)

of water was applied, equivalent to a rainfall event of ca. 68 mm (Rau et al., 2015). Five drips were activated, which were <1 m apart, all fed by water flowing down one flowstone and onto adjacent stalactites (drip sites 1 and 2 of Rutledge et al., 2014, and three adjacent drips). Site 1 (Fig. 1) was sampled for inorganic geochemistry, fluorescent DOM (FDOM) and LC-OCD as reported by Rutledge et al. (2015). The adjacent Site 3 was used for GDGT sampling. A third drip site, Site 5, was used for monitoring drip rate.

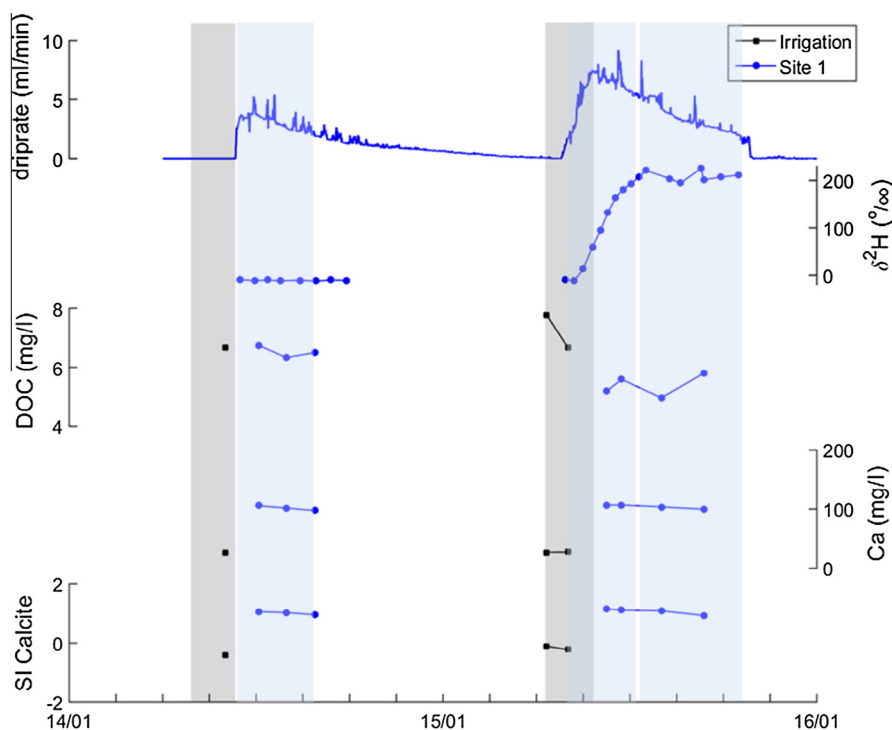


Fig. 2. Drip rate, deuterium ($\delta^2\text{H}$) and selected inorganic geochemistry data (DOC, dissolved organic carbon; Ca, calcium concentration; SI Calcite, saturation index of calcite), for the irrigation water (black squares) and drip water (blue circles) samples. Lines between data points indicate periods of continuous dripping. Grey bars are the periods of irrigation (ca. 68 mm rainfall over 2.85 h in Event 1 and ca. 48 mm over 3 h in Event 2). Blue shaded areas indicate timing of the three GDGT samples. (For interpretation of the references to colour in this figure legend, the reader is referred to the web version of this article.)

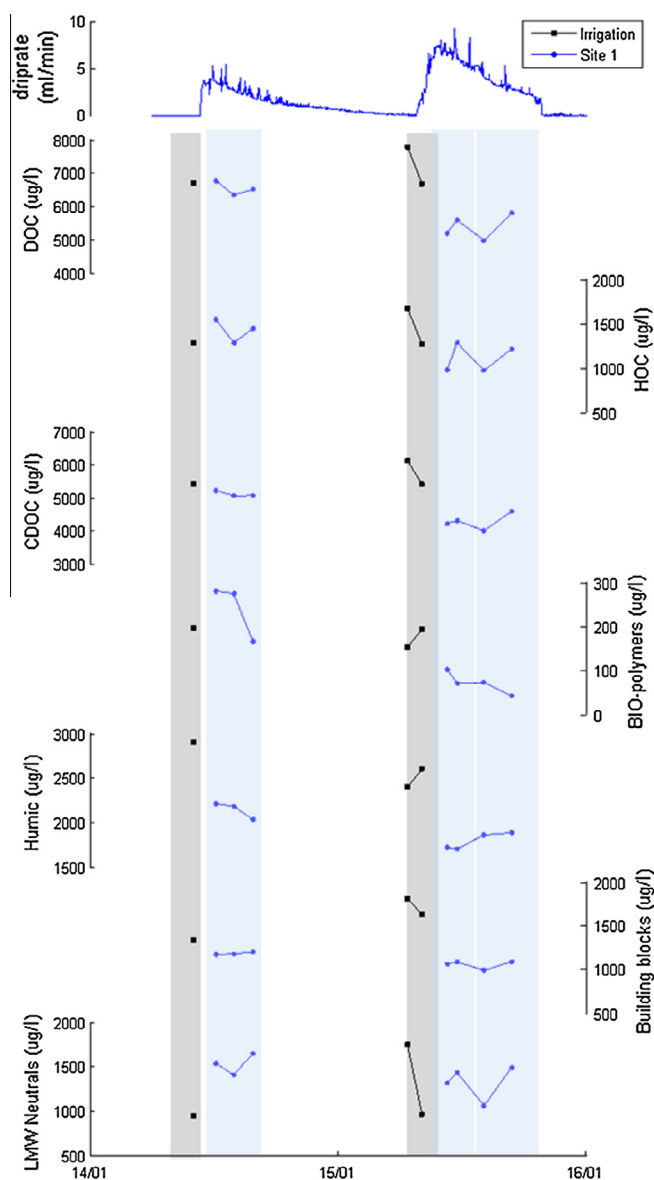


Fig. 4. Time series of LC-OCD fractions (after Rutledge et al., 2015); DOC, dissolved organic carbon; HOC, hydrophobic organic carbon; CDOC, chromophoric dissolved organic carbon; BIO-polymers; humic; building blocks; low molecular weight (LMW) neutrals. See Huber et al. (2011) or Rutledge et al. (2015) for definitions. Lines between data points indicate periods of continuous dripping. Grey shaded areas show timing of irrigation and black squares are irrigation water samples. Blue shaded areas indicate timing of the three GDGT samples. (For interpretation of the references to colour in this figure legend, the reader is referred to the web version of this article.)

The moisture content of the upper 10 cm of soil was $30.9 \pm 5.0\%$ ($n = 10$) at the start of the irrigation on Day 2 (Event 2), which comprised two batches of irrigation water totalling 2400 l. The initial batch was 1100 l town water loaded into a tank on site and spiked with 0.5 l D_2O (99.8%D), resulting in a D enrichment of 6700‰ [vs. Vienna Standard Mean Ocean Water (VSMOW)] as measured using laser cavity ring down mass spectrometry. This batch was hand hosed until all water was used and was followed by a second non-enriched batch of town water. The total irrigation lasted 3 h and was the equivalent of ca. 48 mm rainfall (Rau et al., 2015). This irrigation activated additional drip sites compared with those on Day 1 [not utilised here, but see Rutledge et al. (2015)] and dripping stopped by Day 3.

2.3. GDGT analysis

GDGTs were sampled in 1 l Schott bottles, which had been acid washed, rinsed with dichloromethane (DCM) and additionally capped with DCM-cleaned Al foil. It took several hours for each bottle to fill, with only three drip water samples collected. W-1 was collected within Event 1, from 10:45 until dripping ceased at approximately 03:30 the next morning. W-2 was collected at the first half of Event 2, from 08:00 to 13:00. Sample W-3 was also sampled in Event 2, from 13:00 until dripping ceased at approximately 20:00 that night: a smaller sample was collected as dripping ceased during collection. Samples were also collected from the irrigation water and from a field and laboratory blank. For the latter, the sample bottle was uncapped for 1 h in the cave at drip Site 1, prior to commencement of the irrigation experiment.

The 1 l sample bottles were transported to the lab immediately after collection of sample W-3. They were acidified to pH 2 and extracted using solid phase extraction (SPE) with an all-purpose Agilent Bond Elut C_{18} cartridge (60 ml, 10 g) pre-filled with silica resin. All glassware was acid cleaned and solvent rinsed prior to use. SPE cartridges were pre-rinsed in triplicate, with milli-Q water and conditioned with the eluting solvent. Samples were loaded onto the SPE cartridge on a vacuum manifold and eluted with 60 ml DCM:MeOH (9:1, v:v). Eluents were dried down using rotary evaporation and transferred to 4 ml vials. Each extract was then separated into a non-polar and a polar fraction using a small Al_2O_3 column in a Pasteur pipette, with hexane:DCM (9:1, v:v) and DCM:MeOH (1:1, v:v) as eluent (Schouten et al., 2007). Each polar fraction containing the core GDGTs was dried, redissolved in hexane:isopropanol (99:1, v:v) and filtered over a 0.45 μm PTFE filter.

High performance liquid chromatography–atmospheric pressure chemical ionisation–mass spectrometry (HPLC–APCI–MS) analysis on the core GDGT lipids was carried out with a Thermo Orbitrap XL LC/MSD system using a scan window of m/z 1015–1305 at a resolution of 60,000. The separation of the core GDGTs were performed according to Schouten et al. (2007) using a normal phase Grace Prevail Cyano column (150 mm \times 2.1 mm; 3 μm). The flow rate of the hexane:propanol 99:1 (v/v) eluent was 0.2 ml/min, run isocratically for the first 5 min, thereafter with a linear gradient to 1.8% propanol in 45 min. Injection volume of the samples was 15 μl . For data analysis, 10 ppm wide scan windows were created around the observed m/z values for six iGDGTs (Weijers et al., 2007): GDGT 0 (1302.3227), GDGT 1 (1300.3070), GDGT 2 (1298.2914), GDGT 3 (1296.2757), crenarchaeol (1292.2444) and the nine different brGDGTs [III (1050.0488); IIIb (1048.0306); IIIc (1046.0200); II (1036.0325); IIb (1034.0170); IIc (1032.0044); I (1022.0166); Ib (1020.0017); Ic (1017.9920)]. Peak areas were integrated following the methods described by Schouten et al. (2007) and Weijers et al. (2007); the data were normalised and are reported as fractional abundances and ratios.

2.4. Other hydrogeochemical analyses

Inorganic geochemistry, deuterium (δ^2H), LC-OCD and FDOM analyses have been reported by Rutledge et al. (2015). Only a brief description of a subset of the analyses is provided here, to provide sufficient background information for placing the GDGT data into a broader hydrogeological and geochemical context.

Trace element analysis of the drip water and irrigation samples was carried out using inductively coupled plasma–mass spectrometry (ICP–MS; Perkin Elmer NexION 300D) and optical spectroscopy (ICP–OES; Perkin Elmer Optima 7300). A Dionex ion chromatography system was used to determine the concentration of F^- , Cl^- , NO_2^- , Br^- , NO_3^- , PO_4^{3-} and SO_4^{2-} . Alkalinity was determined in the field by way of Gran titration. PHREEQC for Windows was used to calculate the saturation indices from the element

Table 1
GDGT data for Wellington Caves. Water samples W1–W3 and irrigation water from this study, soil and speleothem data from Blyth et al. (2014). Branched/isoprenoid data for soil and speleothem samples are not provided as the full set of compounds were quantified on different runs, as opposed to a single combined run for the drip water data.

Sample name	Isoprenoid GDGTs		Fractional abundance (%)				Branched GDGTs			Fractional abundance (%)				BIT	Branched/ isoprenoid ratio
	GDGT-0	GDGT-1	GDGT-2	GDGT-3	Cren	Cren isomer	GDGT-IIIa	GDGT-IIa	GDGT-IIb	GDGT-IIC	GDGT-Ia	GDGT-Ib	GRGT-Ic		
	W-1	56.2	10.8	15.0	1.9	12.1	4.0	10.8	43.5	11.2	0.3	28.8	5.5		
W-2	27.2	6.4	11.8	0.3	51.2	3.2	3.7	41.6	15.0	0.5	30.0	7.8	1.3	0.95	11.71
W-3	46.6	7.1	10.9	1.3	33.0	1.1	0.0	41.5	14.8	1.2	29.0	13.4	0.0	0.78	1.65
Irrigation water	20.3	8.4	7.6	5.4	58.2	0.1	0.0	46.4	10.6	0.6	34.2	8.3	0.0	0.92	7.70
Cat-soil-1	15.0	8.3	10.9	4.1	57.2	4.5	11.0	44.3	11.4	0.4	22.2	9.4	0.7	0.52	No data
Cat-soil-2	22.1	4.7	7.7	4.3	53.3	7.9	9.4	47.2	8.4	0.5	24.8	7.3	1.4	0.74	No data
Gad-soil-1	15.4	7.8	10.4	4.5	55.5	6.5	11.7	45.3	9.5	0.3	23.8	8.2	0.6	0.82	No data
Gad-soil-2	13.0	7.2	11.2	5.3	56.2	7.2	11.8	40.2	12.1	0.3	22.1	11.9	0.6	0.80	No data
Wel-C-1	8.9	11.0	10.7	11.9	55.7	1.8	9.5	31.8	26.6	2.7	13.4	12.0	2.0	0.07	No data
Wel-C-2	8.0	9.6	9.8	10.8	58.2	3.7	5.5	25.6	28.2	5.3	14.0	13.8	3.2	0.17	No data
Wel-C-3	8.8	9.9	10.1	12.1	56.6	2.6	8.3	26.2	22.0	4.5	17.6	13.8	4.8	0.27	No data
Wel-G-1	6.9	7.3	6.0	8.7	63.8	7.3	9.7	18.0	20.8	7.2	12.9	21.2	10.1	0.05	No data

concentrations. Only Ca^{2+} concentration and calcite saturation index data are presented.

LC-OCD is an automated size-exclusion chromatography system. The chromatography subdivides a sample into six fractions, which are assigned to specific classes of compounds - biopolymers, humics, building blocks, low molecular weight (LMW) neutrals and hydrophobic OC (Huber et al., 2011). The total amount of dissolved OC is also provided, and the hydrophobic OC is calculated by difference. This fraction contains the GDGTs.

Fluorescence excitation-emission matrices (EEMs) were obtained using a Horiba Aqualog fluorescence spectrometer. Rutledge et al. (2015) demonstrated a strong correlation between the FDOM results and humic and bio-polymer LC-OCD fractions, and FDOM data are therefore not reported again here. The isotopic composition of irrigation and drip water samples was determined using an LGR-100DT V2off-axis, integrated cavity output, cavity ring-down MS system (Lis et al., 2008). Both the hydrogen and oxygen isotopes were analysed, but only the deuterium data are presented here (comprehensive presentation of the isotope data is provided by Markowska et al. 2016).

3. Results and discussion

3.1. Drip water hydrology and geochemistry

Fig. 2 shows the drip rate data over the course of the experiment, in comparison with the inorganic and organic parameters that best define the flow pathways. Dripping at Sites 1, 3 and 5 was activated on Day 1 and stopped on Day 3. The two irrigations above the cave resulted in two significant pulses, with a 3 h delay on Day 1 and 1 h delay on Day 2 from the start of each irrigation. These delayed drip responses are consistent with our hydrological conceptual model for the site, in which soil moisture deficits must be overcome before dripping is activated in the cave beneath the irrigation area. Observed changes in soil moisture are presented in Fig. 3. On Day 1, soil moisture increased from an average of 14.4% to a maximum of 36.5% ca. 5 h after irrigation started, and on Day 2 increased from 30.9 to 36.6% within 2 h of irrigation starting and maintained at above 30% for 24 h, explaining the longer delay between irrigation and drip activation on Day 1.

The irrigation water was only available from the local town water supply, where DOM is at a comparable level to the values in the drip water. Therefore, we had to assess the possibility that DOM in the drip water could be derived from existing DOM in

the town water. Spiking the irrigation water in Event 2 with ^2H allowed us to make a qualitative assessment of the relative origins of DOM in the drip water. Fig. 2 shows that a maximum ^2H enrichment of ca. 200‰, equivalent to <3% of the initial deuteriated water, was present at Site 1, confirming that only a small proportion of DOM would likely be derived from the town supply water. Rutledge et al. (2015) also found distinctly different LC-OCD signatures between town supply water and drip water samples.

Fig. 2 shows that the drip water geochemistry had a greater bedrock signature following Event 2 than Event 1, in agreement with the hydrochemical results from the 2013 irrigation experiment (Rutledge et al., 2014). Bedrock derived trace element concentration, calcite saturation index and Ca^{2+} concentration all increased over time, and DOC decreased (Fig. 2). From the inorganic geochemical response from the 2013 and 2014 irrigation experiments (Rutledge et al., 2014, 2015), we were able to establish a general conceptual model for water movement at the irrigation site.

For the 2014 irrigation reported here, we hypothesise that, in Event 1, a large volume of the irrigation water was absorbed within the relatively unsaturated soil profile, until field capacity was reached (defined as the time when surface water ponding was first observed during the irrigation, which corresponded to a soil moisture >ca. 35%). When water flow to the karst commenced, it is likely that any bedrock fractures and solution features were also relatively dry, due to the dry antecedent conditions. Therefore, the drip water that reached the cave initially had a limited duration of contact with the limestone bedrock and proportionally longer contact time with the deeper soil.

In contrast, Event 2 irrigation water generated dripping in the cave more quickly than Event 1. Residual irrigation water from Event 1 would have been held overnight in subsurface fractures and solution features where the topography enabled this, and irrigation water remaining in the deeper soil profiles would have started to equilibrate with the soil chemistry. The Event 2 irrigation would have very quickly re-saturated the surface soil, and the gradual increase and significant dilution of the deuterium tracer in drip water following Event 2 suggests this comprised an initial pulse of residual water from Event 1.

3.2. OM characterisation: LC-OCD and GDGTs

Fig. 4 shows the time series concentration profiles for the organic fractions measured with LC-OCD. Overall, the DOC at Site

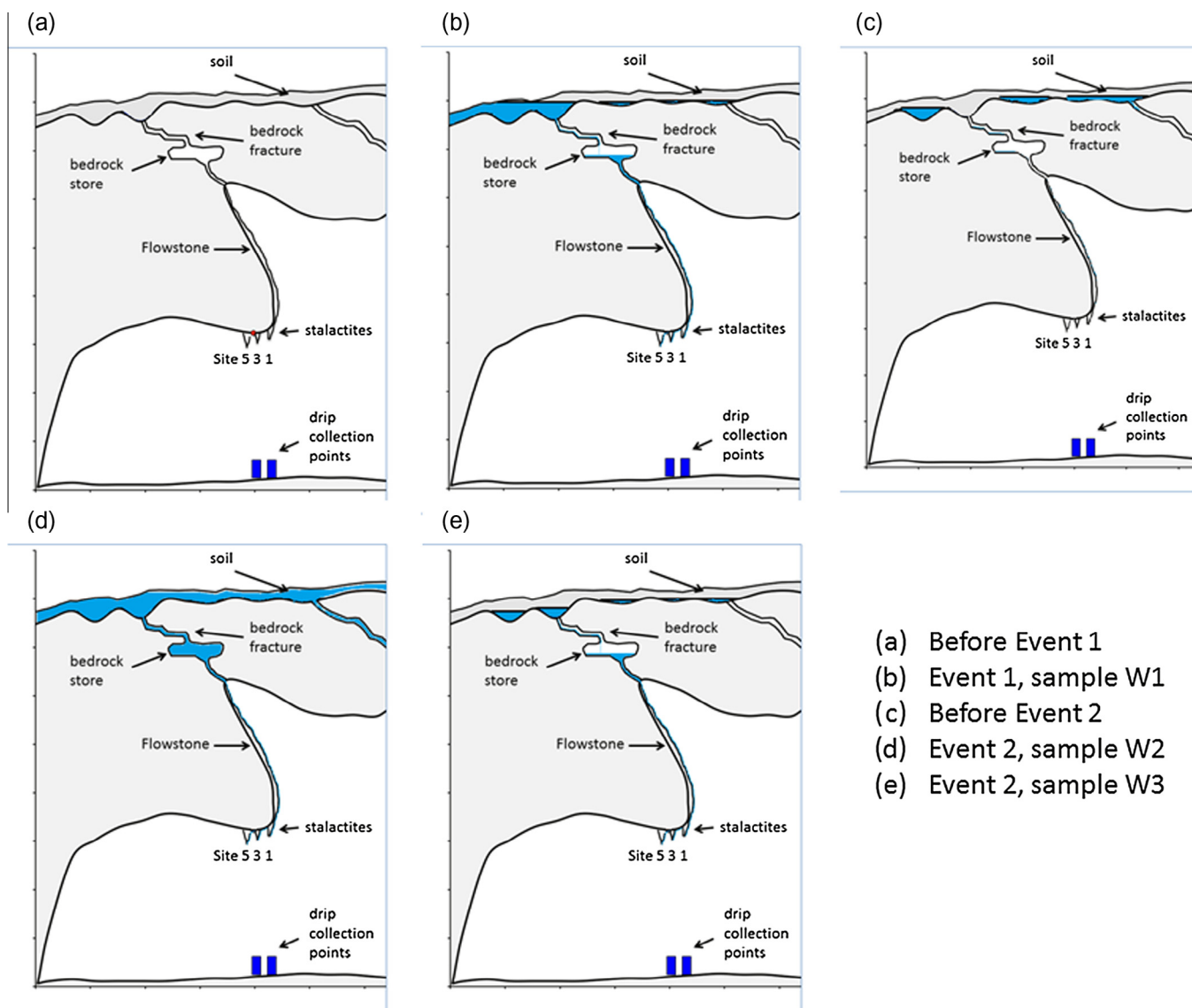


Fig. 5. Drip water flow conceptual model. Although the fractures and water stores are conceptual, the horizontal and vertical tick marks are to scale and represent 1 m.

1 decreased over the course of the irrigation tests. The DOC comprises HOC (hydrophobic) and CDOC (hydrophilic), and CDOC can be further broken down into fractions comprising bio-polymers, humics, building blocks and LMW neutrals. The concentration of CDOC was significantly higher than the HOC concentration, and all fractions showed a step decrease between Event 1 and Event 2. For a detailed analysis of the LC-OCD results see Rutledge et al. (2015). The GDGTs in the drip water would be contained within the HOC fraction.

Table 1 shows the GDGT results. The field and laboratory blank showed GDGTs below detection limit. The ratio of all brGDGTs to iGDGTs increased from 2.85 (following Event 1) to 11.71 (following Event 2, Day 2), before decreasing to 1.65 (Event 2, end of Day 2). The distribution of iGDGTs varied across the three samples in terms of the relative amounts of crenarchaeol and GDGT 0, with a dominance of the latter indicating a methanogenic input (Blaga et al., 2009). The composition was also distinct from that of the irrigation tank sample (Fig. 4), as might be expected, given that <3% of the drip water was shown to be irrigation water. For the brGDGTs, the distribution of the individual compounds exhibited less

variability than the iGDGTs across the three samples, suggesting perhaps a common or a similar bacterial source.

LC-OCD and GDGT results demonstrated contrasting responses to the irrigation experiment. LC-OCD data, demonstrating a broad step decrease in OM concentration from Event 1 to Event 2 across all fractions, reflect in part the decreased contact time with the soil after the second irrigation. It could also demonstrate a first flush of humic-like material from the soil after Event 1, which was then both diluted and potentially partly exhausted during Event 2. In the GDGT distributions, Event 2 showed a marked increase in brGDGTs, as indicated by the increased branched/isoprenoid ratio. A relative increase in the ratio would be expected if there was a greater proportion of soil-derived GDGTs in the drip water, especially from the upper soil surface where the brGDGT abundance is greatest (Naeher et al., 2014; Ajioka et al., 2014). Event 2 also showed a significantly increased input of crenarchaeol relative to other iGDGTs. Crenarchaeol has been proposed to be a specific biomarker for Thaumarchaeota (Damsté et al., 2002), chemoautotrophic Archaea capable of NH_3 oxidation. These Archaea are known to be present in the soil (e.g. Leininger et al. 2006;

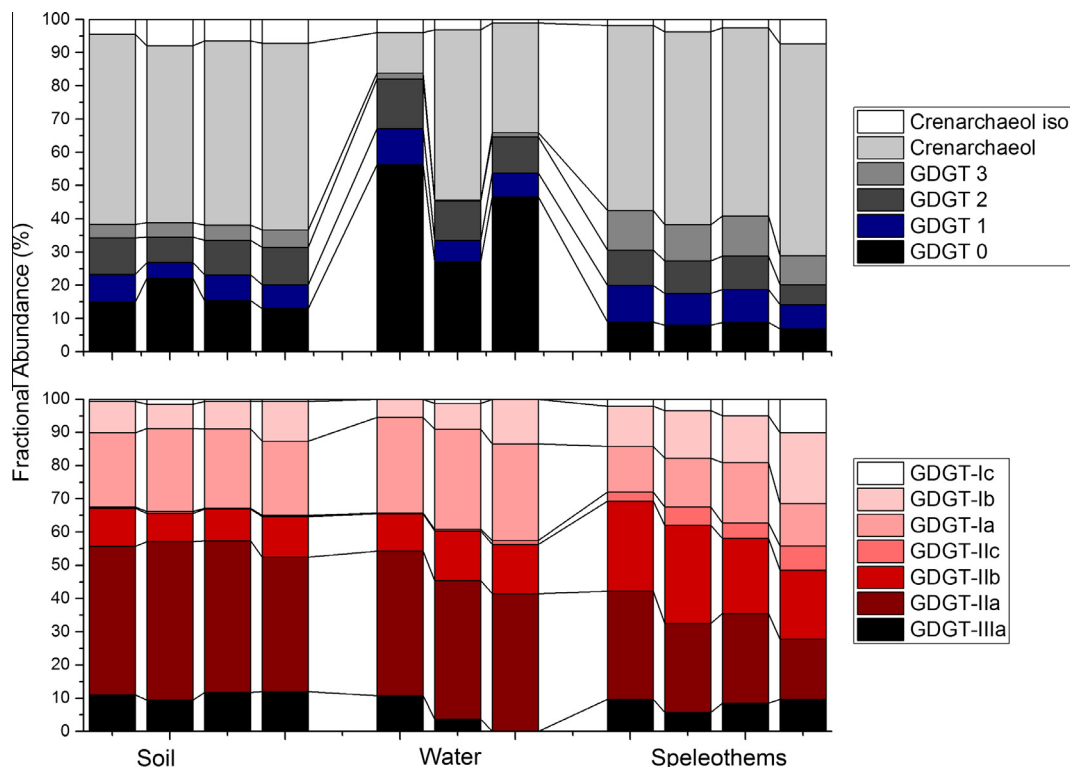


Fig. 6. Comparison of fractional abundance of iGDGTs between drip water, soil and speleothems at Wellington Caves. Soil and speleothem data from Blyth et al. (2014).

Xie et al., 2015) but have yet to be investigated in karst vadose zone or groundwater. Globally, crenarchaeol abundance in soil increases with soil pH (Weijers et al., 2006; Cao et al., 2012) and decreases in abundance with depth (Cao et al., 2012), and Thaumarchaeota have been observed through 16S rRNA analysis in karst cave 'slime curtains' (Tetu et al. 2013), in a silicate cave (Barton et al. 2014) and regional, non-karst groundwater (Flynn et al. 2013).

3.3. Conceptual model of drip water and GDGT evolution

Fig. 5 presents our conceptual model of the processes in our infiltration experiments. Initial conditions are shown in Fig. 5a, with dry conditions and low soil moisture content. In Event 1 (Fig. 5b), drip water has relatively high DOM and low inorganic species associated with limestone dissolution, suggesting a flush of OM from the soil and limited contact with, or storage in, the limestone. GDGTs have a relatively low ratio of brGDGTs/isoprenoid GDGTs compared with Event 2. We hypothesise that the GDGTs derive predominantly from the deeper part of the soil profile, potentially the epikarst.

During and after the second irrigation, drip water flow commences sooner, since there is very little soil moisture deficit to overcome to initiate drainage from the soil to the cave, and is maintained for longer. There is a decrease in DOM concentration compared with the first irrigation, and a slight increase in the geochemical signature from limestone dissolution. Drip water therefore comprises a component that has been in contact with the limestone for longer, which is most likely water stored overnight in karst surface depressions and vadose zone stores (Fig. 5c). In Event 2, the GDGTs have the highest ratio of brGDGTs/iGDGTs. We hypothesise that a greater degree of near-surface saturation and water ponding within Event 2 enables a greater proportion of near surface GDGTs to be present in the drip water in Event 2, despite the overall lower DOC concentration (Fig. 5d). Activation

of preferential flow pathways at high soil moisture content during Event 2 is a likely mechanism that would increase the brGDGTs/iGDGTs by increasing the rate of transport of near surface GDGTs to the cave. On Day 3, we sampled the tail of the hydrograph of Event 2. Any preferential flow pathways connecting to the surface, activated at the start of the event, would now be inactive, since irrigation is no longer happening and drip water geochemical signatures are derived predominantly from drainage from the deeper soil layers and from fractures and stores in the limestone (Fig. 5e). Consequently, the GDGT signature reverts to one with a lower ratio of brGDGTs/iGDGTs.

3.4. Comparison of water, soil and speleothem GDGTs

In Table 1 the GDGT composition of the drip water samples is compared with published data from soils and speleothems sampled above and within two caves at Wellington: Gaden Cave and Cathedral Cave. The soil and speleothem GDGT data are from Blyth et al. (2014) and Blyth and Schouten (2013). All Cathedral Cave soil and speleothem samples were from within 30 m of the irrigation site, with the speleothems sampled from a greater depth below ground surface (ca. 20 m lower) than the irrigation site. It can be seen that the drip water signal is distinctly different from both the soil and speleothems. Drip water samples show a greater similarity to the soil signals, both in the dominance of the branched compounds, and the internal distribution of the brGDGTs (Fig. 6). In the iGDGT fraction, the drip water exhibits much greater GDGT 0 than in soils and speleothems. GDGT 0 is often related to methanotrophic archaea (Schouten et al., 2013) and its high fractional abundance in the dripwater could reflect a local methanogenic microbial community associated with localised perched water stores thought to exist at the site (Cuthbert et al., 2014a).

In the speleothem isoprenoid signal (averaged across 3 samples), there is a strong dominance of crenarchaeol and a higher proportion of GDGT 3 than GDGTs 1 and 2. The difference is more

pronounced in the brGDGTs where the soil and drip water samples all show very similar distributions, while the speleothem samples have a much higher relative proportion of GDGTs Ib and IIb, indicating a high proportion of moieties containing one cyclopentane ring. This increased degree of cyclisation in speleothems relative to soils was noted by Blyth et al. (2014), who showed that it was not related to soil and dripwater pH at the Wellington site.

The results here indicate that the drip water, soil and speleothem signals are also distinct (Fig. 6), suggesting that the control on the increased cyclisation occurs within the karst system, either during infiltration storage and water transport, or within the cave, most likely on the speleothem surface. This in turn suggests that micro-climatic factors and variation in cave and karst microbiology may significantly control the GDGT signal within speleothems. This is important in the potential use of proxies based on isoprenoid tetraethers (TEX₈₆) or branched tetraethers (MBT/CBT) in speleothems to develop palaeotemperature records. Although it has been shown that both iGDGT and brGDGT distributions in speleothems have statistically significant relationships with surface air temperature (Blyth and Schouten 2013), the findings presented here further illustrate the need for investigation of in-cave variation and recalibration of the proxy to cave temperature values. Barton et al. (2014) used a cave in a nutrient-limited, orthosilicate geology to suggest that it is the water entering the cave that provides the carbon and energy necessary for within-cave microbial community growth and subsistence. Recent long term monitoring of drip water bacterial communities at Heshang cave, China, provides the first insight into the possible characteristics of a microbial source of GDGTs in drip water (Yun et al., 2015). Future research could also consider the analysis of both core lipids and intact polar lipids in soils, drip water and speleothems, as undertaken for marine sediment cores (Lengger et al., 2012). Comparison of core and intact polar lipids would permit the investigation of the relative abundance of GDGT lipids from soil to speleothem with respect to their relative solubility.

4. Conclusions

The use of an artificial irrigation experiment using multiple tracers has further elucidated the potential source of GDGTs in speleothems. We observed limited similarity in GDGT composition between soil, water and speleothem samples. We observed an increase in brGDGTs in the drip water when we fully saturated the overlying soil, but the composition of these brGDGTs was distinctly different from GDGTs extracted directly from soils. Speleothem GDGT composition was different again from soil and drip water, both in brGDGTs/iGDGT ratio and GDGT composition. These experimental findings provide further evidence that the speleothem GDGT signature was likely to be modified by a within-cave microbial source. Given the differences in GDGT composition, a within-cave calibration of the GDGT–temperature relationship should be more appropriate than a soil GDGT–temperature relationship. We note that our site, relatively near the cave entrance and shallow, would be one that would favour a soil-derived GDGT signal, but yet this was not observed. Further experiments comparing drip water and speleothem GDGTs at deeper cave sites, and over the hydrological cycle, should be informative for further constraining our understanding of the speleothem GDGT signature.

Acknowledgements

We thank the staff at Wellington Caves for their support. Funding was provided by the Australian Research Council (ARC; DP110102124) and the National Centre for Groundwater Research and Training, an Australian Government Initiative, supported by

the ARC and the National Water Commission. A.J.B. acknowledges the support of an AINSE Research Fellowship and Curtin University. M.O.C. was supported by Marie Curie Research Fellowship funding from the European Community's Seventh Framework Programme (FP7/2007–2013) under grant agreement n°299091. The Connected Waters Initiative Research Centre acknowledges funding from G. Johnston. We thank the Sydney University Speleological Society for provision of the cave survey information used in Fig. 1 and two anonymous reviewers for comments.

Associate Editor—S. Schouten

References

- Ajioka, T., Yamamoto, M., Murase, J., 2014. Branched and isoprenoid glycerol dialkyl glycerol tetraethers in soils and lake/river sediments in Lake Biwa basin and implications for MBT/CBT proxies. *Organic Geochemistry* 73, 70–82.
- Baker, A., Barnes, W.L., Smart, P.L., 1997. Stalagmite drip discharge and organic matter fluxes in Lower Cave, Bristol. *Hydrological Processes* 11, 1541–1555.
- Barton, H.A., Giarrizzo, J.G., Suarez, P., Robertson, C.E., Broering, M.J., Banks, E.D., Vaishampayan, P.A., Venkateswaran, K., 2014. Microbial diversity in a Venezuelan orthoquartzite cave is dominated by *Chloroflexi* (Class *Ktedonobacterales*) and Thaumarchaeota Group 1.1c. *Frontiers in Microbiology* 5, 615.
- Blaga, C.I., Reichart, G.J., Heiri, O., Sinninghe Damsté, J.S., 2009. Tetraether membrane lipid distributions in lake particulate matter and sediments: a study of 47 European lakes along a North-South transect. *Journal of Paleolimnology* 41, 523–540.
- Blyth, A.J., Watson, J.S., 2009. Thermochemolysis of organic matter preserved in stalagmites: a preliminary study. *Organic Geochemistry* 40, 1029–1031.
- Blyth, A.J., Asrat, A., Baker, A., Gulliver, P., Leng, M.J., Genty, D., 2007. A new approach to detecting vegetation and land-use change using high-resolution lipid biomarker records in stalagmites. *Quaternary Research* 68, 314–324.
- Blyth, A.J., Baker, A., Collins, M.J., Penkman, K.E.H., Gilmour, M.A., Moss, J.S., Genty, D., Drysdale, R.N., 2008. Molecular organic matter in speleothems and its potential as an environmental proxy. *Quaternary Science Reviews* 27, 905–921.
- Blyth, A.J., Watson, J.S., Woodhead, J., Hellstrom, J., 2010. Organic compounds preserved in a 2.9 million year old stalagmite from the Nullarbor Plain, Australia. *Chemical Geology* 79, 101–105.
- Blyth, A.J., Thomas, L.E., Calsteren, P.V., Baker, A., 2011. A 2000 year lipid biomarker record preserved in a stalagmite from NW Scotland. *Journal of Quaternary Science* 26, 326–334.
- Blyth, A.J., Shutova, Y., Smith, C.I., 2013a. $\delta^{13}\text{C}$ analysis of bulk organic matter in speleothems using liquid chromatography–isotope ratio mass spectrometry. *Organic Geochemistry* 55, 22–25.
- Blyth, A.J., Smith, C.I., Drysdale, R.N., 2013b. A new perspective on the $\delta^{13}\text{C}$ signal preserved in speleothems using LC-IRMS analysis of bulk organic matter and compound specific stable isotope analysis. *Quaternary Science Reviews* 75, 143–149.
- Blyth, A.J., Schouten, S., 2013. Calibrating the glycerol dialkyl glycerol tetraether temperature signal in speleothems. *Geochimica et Cosmochimica Acta* 109, 312–328.
- Blyth, A.J., Jex, C., Baker, A., Khan, S.J., Schouten, S., 2014. Contrasting distributions of glycerol dialkyl glycerol tetraethers (GDGTs) in speleothems and associated soils. *Organic Geochemistry* 69, 1–10.
- Bureau of Meteorology, 2015. Monthly Climate Statistics, Wellington Research Centre. <http://www.bom.gov.au/climate/averages/tables/cw_065035_All.shtml> (last accessed 10.08.15).
- Cao, P., Zhang, L.-M., Shen, J.-P., Zheng, Y.-M., Di, H.J., He, J.-Z., 2012. Distribution and diversity of archaeal communities in selected Chinese soils. *FEMS Microbiology Ecology* 80, 146–158.
- Cuthbert, M.O., Baker, A., Jex, C.N., Graham, P., Treble, P., Andersen, M.S., Acworth, R. I., 2014a. Drip water isotopes in semi-arid karst: implications for speleothem paleoclimatology. *Earth and Planetary Science Letters* 395, 194–204.
- Cuthbert, M.O., Rau, G.C., Andersen, M.S., Roshan, H., Rutledge, H., Marjo, C.E., Markowska, M., Graham, P.W., Mariethoz, G., Baker, A., 2014b. Evaporative cooling of speleothem drip water. *Scientific Reports* 4 5162.
- Damsté, J.S., Schouten, S., Hopmans, E.C., van Duin, A.C., Geenevasen, J.A., 2002. Crenarchaeol: the characteristic core glycerol dibiphytanyl glycerol tetraether membrane lipid of cosmopolitan pelagic crenarchaeota. *Journal of Lipid Research* 43, 1641–1651.
- Fairchild, I.J., Baker, A., 2012. *Speleothem Science*. Wiley-Blackwell.
- Flynn, T.M., Sanford, R.A., Ryu, H., Bethke, C.M., Levine, A.D., Ashbolt, N.J., Domingo, J.W.S., 2013. Functional microbial diversity explains groundwater chemistry in a pristine aquifer. *BMC Microbiology* 13, 146.
- Frank, R., 1971. *The clastic sediments of the Wellington Caves, New South Wales*. *Helveticite* 9, 3–26.
- Hartland, A., Fairchild, I.J., Lead, J.R., Borsato, A., Baker, A., Frisia, S., Baalousha, M., 2012. From soil to cave: transport of trace metals by natural organic matter in cave dripwaters. *Chemical Geology* 304–305, 68–82.
- Hesse, P.P., McTainsh, G.H., 2003. Australian dust deposits: modern processes and the Quaternary record. *Quaternary Science Reviews* 22, 2007–2035.

- Huber, S.A., Balz, A., Abert, M., Pronk, W., 2011. Characterisation of aquatic humic and non-humic matter with size-exclusion chromatography – organic carbon detection – organic nitrogen detection (LC-OCD-OND). *Water Research* 45, 879–885.
- Huguet, A., Francez, A.-J., Jusselme, M.D., Fosse, C., Derenne, S., 2014. A climatic chamber experiment to test the short term effect of increasing temperature on branched GDGT distribution in Sphagnum peat. *Organic Geochemistry* 73, 109–112.
- Jex, C.N., Mariethoz, G., Baker, A., Graham, P., Andersen, M.S., Acworth, I., Edwards, N., Azcurra, C., 2012. Spatially dense drip hydrological monitoring at the Wellington Caves, South East Australia. *International Journal of Speleology* 41, 285–298.
- Johnson, B.D., 1975. The Garra Formation (early Devonian) at Wellington, N.S.W. *Journal and Proceedings of the Royal Society of New South Wales* 108, 111–118.
- Leininger, S., Ulrich, T., Schwark, L., Qi, J., Nicol, G.W., Prosser, J.L., Schuster, S.C., Schleper, C., 2006. Archaea predominate among ammonia-oxidising prokaryotes in soils. *Nature* 442, 806–809.
- Lengger, S.K., Hopmans, E.C., Reichart, G.-J., Nierop, K.G.J., Damsté, J.S., Schouten, S., 2012. Intact polar and core glycerol diphytanyl glycerol tetraether lipids in the Arabian Sea oxygen minimum zone. Part II: selective preservation and degradation in sediments and consequences for the TEX₈₆. *Geochimica et Cosmochimica Acta* 98, 244–258.
- Li, X., Hu, C., Huang, J., Xie, S., Baker, A., 2014. A 9000-year carbon isotopic record of acid-soluble organic matter in a stalagmite from Heshang Cave, central China: implication for paleoclimate implications. *Chemical Geology* 388, 71–77.
- Lis, G.P., Wassenaar, L.I., Hendry, M.J., 2008. High-precision laser spectroscopy D/H and ¹⁸O/¹⁶O measurements of microliter natural water samples. *Analytical Chemistry* 80, 287–293.
- Markowska, M., Baker, A., Andersen, M.S., Jex, C.N., Cuthbert, M.O., Rau, G.C., Graham, P.W., Rutledge, H., Mariethoz, G., Marjo, C.E., Treble, P.C., Edwards, N., 2016. Semi-arid caves: evaporation and hydrological controls on $\delta^{18}\text{O}$ drip water composition and implications for speleothem paleoclimate reconstructions. *Quaternary Science Reviews* 131, 285–301.
- Naeher, S., Peterse, F., Smittenburg, R.H., Niemann, H., Zigah, P.K., Schubert, C.J., 2014. Sources of glycerol dialkyl glycerol tetraethers (GDGTs) in catchment soils, water column and sediments of Lake Rotsee (Switzerland) – Implications for the application of GDGT-based proxies for lakes. *Organic Geochemistry* 6, 164–173.
- Peterse, F., van der Meer, M.T.J., Schouten, S., Weijers, J.W.H., Fierer, N., Jackson, R.B., Kim, J.-H., Sinninghe Damsté, J.S., 2012. Revised calibration of the MBT-CBT paleotemperature proxy based on branched tetraether membrane lipids in surface soils. *Geochimica et Cosmochimica Acta* 96, 215–229.
- Rau, G.C., Cuthbert, M.O., Andersen, M.S., Baker, A., Rutledge, H., Markowska, M., Roshan, H., Marjo, C.E., Graham, P.W., Acworth, R.I., 2015. Controls on cave drip water temperature and implications for speleothem-based paleoclimate reconstructions: from surface to drip source. *Quaternary Science Reviews* 127, 19–36.
- Rushdi, A.I., Clark, P.U., Mix, A.C., Ersek, V., Simoneit, B.R.T., Cheng, H., Edwards, R.L., 2011. Composition and sources of lipid compounds in speleothem calcite from southwestern Oregon and their paleoenvironmental implications. *Environmental Earth Sciences* 62, 1245–1261.
- Rutledge, H., Baker, A., Marjo, C.E., Andersen, M.S., Graham, P., Cuthbert, M.O., Rau, G.C., Roshan, H., Markowska, M., Mariethoz, G., Jex, C., 2014. Dripwater organic matter and trace element geochemistry in a semi-arid karst environment: implications for speleothem paleoclimatology. *Geochimica et Cosmochimica Acta* 135, 217–230.
- Rutledge, H., Andersen, M.S., Baker, A., Chinu, K.J., Cuthbert, M.O., Marjo, C.E., Markowska, M., Jex, C.N., Rau, G.C., 2015. Organic characterisation of cave drip water by LC-OCD and fluorescence analysis. *Geochimica et Cosmochimica Acta* 166, 15–28.
- Schouten, S., Huguet, C., Hopmans, E.C., Kienhuis, M.V.M., Sinninghe Damsté, J.S., 2007. Analytical methodology for TEX₈₆ paleothermometry by high-performance liquid chromatography/atmospheric pressure chemical ionization-mass spectrometry. *Analytical Chemistry* 79, 2940–2944.
- Schouten, S., Hopmans, E.C., Sinninghe Damsté, J.S., 2013. The organic geochemistry of glycerol dialkyl glycerol tetraether lipids: a review. *Organic Geochemistry* 54, 19–61.
- Tetu, S.G., Breakwell, K., Elbourne, L.D.H., Holmes, A.J., Gillings, M.R., Paulsen, I.T., 2013. Life in the dark: metagenomics evidence that a microbial slime community is driven by inorganic nitrogen metabolism. *The ISM Journal* 7, 1227–1236.
- Weijers, J.W.H., Schouten, S., Spaargaren, O.C., Sinninghe Damsté, J.S., 2006. Occurrence and distribution of tetraether membrane lipids in soils: implications for the use of the TEX₈₆ proxy and the BIT index. *Organic Geochemistry* 37, 1680–1693.
- Weijers, J.W.H., Schouten, S., van den Donker, J.C., Hopmans, E.C., Sinninghe Damsté, J.S., 2007. Environmental controls on bacterial tetraether membrane lipid distribution in soils. *Geochimica et Cosmochimica Acta* 71, 703–713.
- Weijers, J.W.H., Wiesenberg, G.L.B., Bol, R., Hopmans, E.C., Pancost, R.D., 2010. Carbon isotopic composition of branched tetraether membrane lipids in soils suggest a rapid turnover and a heterotrophic life style of their source organism (s). *Biogeosciences* 7, 2959–2973.
- Xie, S., Yi, Y., Huang, J., Hu, C., Cai, Y., Collins, M., Baker, A., 2003. Lipid distribution in a subtropical southern China stalagmite as a record of soil ecosystem response to paleoclimate change. *Quaternary Research* 60, 340–347.
- Xie, W., Zhang, C., Ma, C., 2015. Temporal variation in community structure and lipid composition of Thaumarchaeota from subtropical soil: insight into proposing a new soil pH proxy. *Organic Geochemistry* 83/84, 54–64.
- Yang, H., Ding, W., Zhang, C.L., Wu, X., Ma, X., He, G., Huang, J., Xie, S., 2011. Occurrence of tetraether lipids in stalagmites: implications for sources and GDGT-based proxies. *Organic Geochemistry* 42, 108–115.
- Yun, Y., Xiang, X., Wang, H., Man, B., Gong, L., Liu, Q., Dong, Q., Wang, R., 2015. Five-year monitoring of bacterial communities in dripping water from the Heshang Cave in Central China: implications for paleoclimate reconstruction and ecological functions. *Geomicrobiology Journal* 1018. <http://dx.doi.org/10.10180/01490451.2015.1062062>.